IDH1 deficiency attenuates gluconeogenesis in mouse liver by impairing amino acid utilization

Jing Ye[a,b,1,2], Yu Gu[a,b,1], Feng Zhang[b,1], Yuanlin Zhao[b], Yuan Yuan[b], Zhenyue Hao[a], Yi Sheng[a], Wanda Y. Li[a], Andrew Wakeham[a], Rob A. Cairns[a], and Tak W. Mak[a,2]

[a]The Campbell Family Institute for Breast Cancer Research, Ontario Cancer Institute, University Health Network, Toronto, ON, Canada M5G 2C1; and [b]Department of Pathology and Pathophysiology, Fourth Military Medical University, Xi'an 710032, China

Contributed by Tak W. Mak, November 18, 2016 (sent for review September 12, 2016; reviewed by Jorge Moscat and Karen H. Vousden)

Although the enzymatic activity of isocitrate dehydrogenase 1 (IDH1) was defined decades ago, its functions in vivo are not yet fully understood. Cytosolic IDH1 converts isocitrate to α-ketoglutarate (α-KG), a key metabolite regulating nitrogen homeostasis in catabolic pathways. It was thought that IDH1 might enhance lipid biosynthesis in liver or adipose tissue by generating NADPH, but we show here that lipid contents are relatively unchanged in both *IDH1*-null mouse liver and *IDH1*-deficient HepG2 cells generated using the CRISPR-Cas9 system. Instead, we found that IDH1 is critical for liver amino acid (AA) utilization. Body weights of *IDH1*-null mice fed a high-protein diet (HPD) were abnormally low. After prolonged fasting, *IDH1*-null mice exhibited decreased blood glucose but elevated blood alanine and glycine compared with wild-type (WT) controls. Similarly, in *IDH1*-deficient HepG2 cells, glucose consumption was increased, but alanine utilization and levels of intracellular α-KG and glutamate were reduced. In *IDH1*-deficient primary hepatocytes, gluconeogenesis as well as production of ammonia and urea were decreased. In *IDH1*-deficient whole livers, expression levels of genes involved in AA metabolism were reduced, whereas those involved in gluconeogenesis were up-regulated. Thus, IDH1 is critical for AA utilization in vivo and its deficiency attenuates gluconeogenesis primarily by impairing α-KG–dependent transamination of glucogenic AAs such as alanine.

isocitrate dehydrogenase 1 | α-ketoglutarate | gluconeogenesis | transamination | liver

Isocitrate dehydrogenases (IDH) convert isocitrate to α-ketoglutarate (α-KG) by reducing $NADP^+$ or NAD^+. The recent discovery of IDH1 and IDH2 mutations in human cancers (1–4) has elicited new interest in defining IDH1's functions in vivo, which are still poorly understood. IDH1 is abundant in liver and was reported to participate in lipid biosynthesis in hepatocyte cytoplasm and peroxisomes (5, 6). Mutant mice overexpressing IDH1 in liver and adipose tissue are obese, have fatty livers, and show elevated plasma triglycerides (TG) and cholesterol (7). In tumor cells, IDH1 contributes to de novo lipogenesis by generating acetyl-CoA building blocks via the NADPH-dependent reductive carboxylation of α-KG to isocitrate (8–11). However, *IDH1*-null mice at steady-state are healthy and fertile, maintain normal body weight, and show no inflammatory symptoms (12).

The liver maintains normal blood glucose levels through glycogenolysis and gluconeogenesis. Gluconeogenesis generates glucose from noncarbohydrate carbon substrates such as pyruvate, lactate, glycerol, and glucogenic amino acids (AAs). During prolonged fasting, the breakdown of skeletal muscle generates limited carbon resources in the form of AAs such as alanine. Hence, both fasting and feeding of a high-protein diet (HPD) can stimulate AA deamination and urea production in the liver (13), where AA carbon skeletons are converted into glucose or lipids. For most AAs, the amino group is transferred to α-KG to generate glutamate and other α-keto acids. For example, alanine from blood or skeletal muscle can be transaminated to form pyruvate in hepatocyte cytosol. After transport into mitochondria, glutamate is oxidatively deaminated by glutamate dehydrogenase 1 (GLUD1) to produce α-KG and toxic ammonia. Ammonia is then eliminated via the urea cycle in the liver. Cytosolic α-KG produced by IDH1 is thus an important nitrogen transporter and prevents nitrogen overload (Fig. 1). However, precisely how IDH1 functions in this process is unknown. In this study, we use *IDH1*-null mice and *IDH1*-deficient HepG2 cells to explore the roles of IDH1 in hepatic nitrogen metabolism and gluconeogenesis.

Results

IDH1 Deficiency Reduces Body Weight Gain and Fasting Blood Glucose in Mice. Immunoblotting of WT mouse tissues revealed that IDH1 is abundant in liver, kidney, intestinal mucosa, white adipose tissues (WAT), and brown adipose tissues (BAT). IDH1 is also present at moderate levels in spleen, brain, and heart but is undetectable in skeletal muscle (Fig. 2*A*), consistent with reported mRNA expression patterns in GEO databases (GDS3113). To explore the role of IDH1 in nitrogen metabolism, newly weaned WT and *IDH1*-null mice were fed either a normal diet (ND) of standard chow or an HPD (50% protein), and body weights were recorded 2 times per wk for 8 wk. No significant differences were found in body weights of ND-fed WT and *IDH1*-null mice (Fig. 2*B*). However, the body weights of HPD-fed *IDH1*-null mice were significantly lower than those of HPD-fed WT mice after 6 wk on HPD (Fig. 2*C*). By 8 wk, the total amount of epididymal, inguinal, and perirenal WAT was decreased in both HPD-fed WT and *IDH1*-null mice compared with ND-fed mice, but no significant differences occurred between WT and *IDH1*-null mice (Fig. 2*D*). Furthermore, the lipid contents of WT and *IDH1*-null mouse embryonic fibroblasts (MEFs) induced to undergo adipocyte differentiation in vitro were comparable (Fig. S1). We then monitored blood glucose under ND-fed, HPD-fed, and fasting conditions. Although blood

Significance

Isocitrate dehydrogenase 1 (IDH1) is abundant in liver. Although it was reported that IDH1 participates in lipid biosynthesis, we show here that IDH1 is instead critical for hepatic amino acid (AA) utilization. IDH1 catalyzes the generation of cytosolic α-ketoglutarate, which can be converted to glutamate in the liver via transamination. Both *IDH1*-null liver and *IDH1*-deficient HepG2 cells show defects in AA utilization. Because IDH1 mutations occur in various tumors and AA metabolism is critical for tumor cell growth, our elucidation of the functions of wild-type IDH1 in AA utilization should advance our understanding of how mutant IDH promotes malignancy.

Author contributions: J.Y., Y.G., R.A.C., and T.W.M. designed research; J.Y., Y.G., F.Z., Y.Z., Y.Y., Z.H., Y.S., W.Y.L., and A.W. performed research; J.Y., Y.G., F.Z., Y.Z., Y.Y., Z.H., Y.S., W.Y.L., and A.W. analyzed data; and J.Y., Y.G., R.A.C., and T.W.M. wrote the paper.

Reviewers: J.M., Sanford–Burnham Medical Research Institute; and K.H.V., Cancer Research UK Beatson Institute.

The authors declare no conflict of interest.

Freely available online through the PNAS open access option.

[1]J.Y., Y.G., and F.Z. contributed equally to this work.

[2]To whom correspondence may be addressed. Email: tmak@uhnres.utoronto.ca or yejing@fmmu.edu.cn.

This article contains supporting information online at www.pnas.org/lookup/suppl/doi:10.1073/pnas.1618605114/-/DCSupplemental.

www.pnas.org/cgi/doi/10.1073/pnas.1618605114

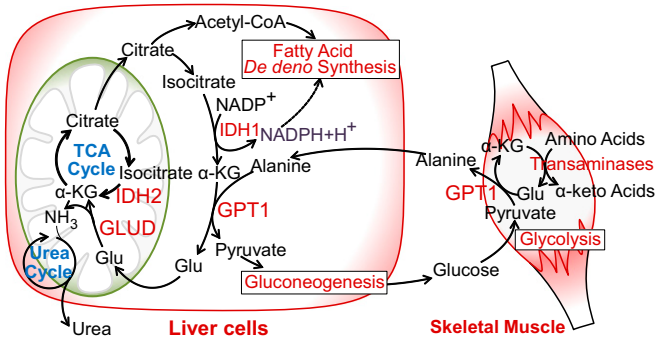

Fig. 1. The potential roles of IDH1 in liver. During prolonged fasting, the breakdown of skeletal muscle generates limited carbon resources in the form of amino acids, mainly alanine. In liver, alanine released from skeletal muscle can be transaminated to form pyruvate using the cytosolic α-KG as the amino acceptor. Thus, the cytosolic α-KG produced by IDH1 is an important nitrogen transporter and prevents nitrogen overload.

glucose levels were similar in ND- and HPD-fed WT and *IDH1*-null mice, they were significantly decreased in *IDH1*-null mice compared with WT controls after fasting for 24 or 48 h after feeding with ND (Fig. 2*E*) or HPD (Fig. 2*F*). Survival of *IDH1*-null mice under prolonged fasting conditions was also impaired (Fig. 2*G*). Thus, IDH1 is important for normal weight gain and blood glucose maintenance.

IDH1 Deficiency Increases Glucose Consumption in HepG2 Cells. To dissect IDH1's biological and metabolic functions, we generated *IDH1*-deficient HepG2 (*IDH1*$^{-}$ HepG2) cells using the CRISPR-Cas9 system (14). Immunoblotting confirmed that endogenous IDH1 was undetectable in *IDH1*$^{-}$ HepG2 cells (Fig. 3*A*). Because hepatic lipids are elevated in *IDH1*-transgenic mice (7), we analyzed lipid contents and glucose consumption in *IDH1*$^{-}$ HepG2 cells. Although *IDH1* loss did not significantly affect lipid content in HepG2 cells (Fig. S2), *IDH1*$^{-}$ HepG2 cells did consume more glucose than *IDH1*$^{+}$ HepG2 cells (Fig. 3*B*). When *IDH1*$^{+}$ and *IDH1*$^{-}$ HepG2 cells were cultured in medium containing abundant (25 mM) glucose, both lines grew to high cell density and showed similar cellular morphology. However, in DMEM with low (5.5 mM) glucose, *IDH1*$^{-}$ HepG2 cells shrank and died as density increased, whereas *IDH1*$^{+}$ HepG2 cells grew well (Fig. 3*C*). When we examined the growth curves of *IDH1*$^{+}$ and *IDH1*$^{-}$ HepG2 cells cultured in medium containing 25 mM glucose, there were no deficits in proliferation or viability (Fig. 3*D*, *Left*). However, after 6 d in medium with 5.5 mM glucose, the growth of *IDH1*$^{-}$ HepG2 cells slowed, and their viability was significantly less than that of *IDH1*$^{+}$ HepG2 cells (Fig. 3*D*, *Right*). Thus, IDH1 is critical for normal glucose consumption and cell growth.

IDH1 Deficiency Increases Plasma AAs. The liver is crucial for lipid and nitrogen metabolism as well as for glucose metabolism. HE and PAS staining of livers of *IDH1*-null mice showed that IDH1 deficiency does not significantly affect hepatocyte morphology or glycogen content (Fig. S3 *A* and *B*). Similarly, Oil Red O staining and TG quantitation indicated that IDH1 loss does not alter hepatic lipid contents (Fig. S3 *C* and *D*), a result confirmed in *IDH1*-null primary hepatocytes (Fig. S3*E*).

To determine the role of IDH1 in nitrogen metabolism, we analyzed blood AAs using LC/MS-MS. Total blood AAs were increased ∼10% in *IDH1*-null mice compared with WT controls under ND-fed or fasting conditions (Fig. 4*A*). However, the blood alanine level in fasted *IDH1*-null mice was significantly elevated compared with fasted WT mice (Fig. 4*B*), whereas blood glycine in both ND-fed and fasted *IDH1*-null mice was increased significantly compared with ND-fed WT mice (Fig. 4*C*). Blood glutamine was higher in *IDH1*-null mice than in WT controls under ND-fed, but not fasting, conditions (Fig. 4*D*).

In the liver, the amino groups of AAs are removed to create α-keto acids that enter the metabolic mainstream as glucose precursors or Krebs cycle intermediates. Because free ammonia is toxic, liver enzymes convert ammonia to urea via the urea cycle. We found that plasma ammonia was decreased in fasted *IDH1*-null mice compared with fasted WT controls but that there was no difference under ND-fed conditions (Fig. 4*E*). Plasma urea levels were comparable to the WT in both ND-fed and fasted *IDH1*-null mice (Fig. 4*F*). Thus, IDH1 in liver is important for the maintenance of normal blood AAs.

IDH1 Deficiency Reduces AA Utilization. We next studied AA utilization in *IDH1*$^{-}$ HepG2 cells. The results revealed that alanine uptake was slowed in *IDH1*$^{-}$ HepG2 cells compared with *IDH1*$^{+}$ HepG2 cells (Fig. 5*A*), but the consumption of glutamine was similar (Fig. S4*A*). In addition, the growth and viability of *IDH1*$^{-}$ HepG2 cells cultured in medium supplemented with 10 mM alanine but lacking glucose was significantly decreased compared with *IDH1*$^{+}$ HepG2 cells (Fig. 5*B*). These results mirrored those obtained when *IDH1*$^{-}$ HepG2 cells were grown in low-glucose medium, again suggesting that alanine utilization is impaired in the absence of IDH1.

We then cultured *IDH1*$^{+}$ and *IDH1*$^{-}$ HepG2 cells in DMEM supplemented with 5% (vol/vol) dialyzed FBS plus various concentrations of glucose or various AAs. When the medium contained >2 mM glucose, *IDH1*$^{-}$ HepG2 cells showed normal viability (Fig. 5*C*, *Left*). However, when the medium contained no glucose but was supplemented with glutamine, alanine, pyruvate, aspartate, glutamate, branch chained amino acids (BCAA), or proline, *IDH1*$^{-}$ HepG2 cells were less viable than *IDH1*$^{+}$ HepG2 cells (Fig. 5*C* and Fig. S4*B*). These results suggest that AAs alone are an insufficient carbon source for the growth of *IDH1*-deficient cells.

Because serum proteins can be used as nitrogen and carbon sources, we cultured HepG2 cells in DMEM without FBS and

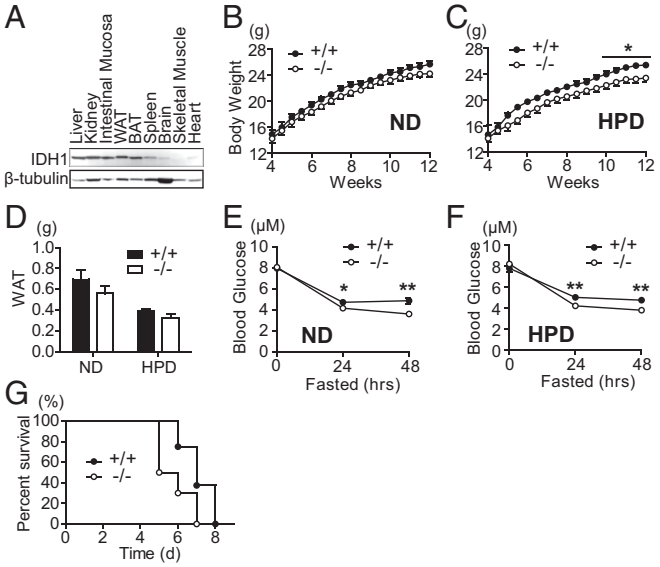

Fig. 2. Decreased blood glucose in *IDH1*-deficient mice subjected to fasting. (*A*) Immunoblot to detect IDH1 in the indicated WT mouse tissues (30 μg protein per well). β-tubulin, loading control. Body weight determinations of newly weaned WT ($^{+/+}$) and *IDH1*-null ($^{-/-}$) mice fed (*B*) an ND of standard chow ($^{+/+}$, $n = 7$; $^{-/-}$, $n = 11$) or (*C*) an HPD ($^{+/+}$, $n = 8$; $^{-/-}$, $n = 9$), for the indicated times. Data are the mean ± SEM. (*D*) Quantitation of total weights of isolated epididymal, inguinal plus perirenal WAT in WT and *IDH1*-null mice fed ND ($n = 8$) or HPD ($n = 8$) for 8 wk. Data are the mean ± SEM. Quantitation of blood glucose levels in WT and *IDH1*-null mice fed either (*E*) ND or (*F*) HPD for 8 wk ($n = 8$). Data are the mean ± SEM. (*G*) Kaplan–Meier analysis of the survival of WT ($n = 10$) and *IDH1*-null ($n = 10$) mice deprived of food but supplied with water ad libitum. For *A*–*G*, $^{*}P < 0.05$, $^{**}P < 0.01$, and $^{***}P < 0.001$ by Student's *t* test.

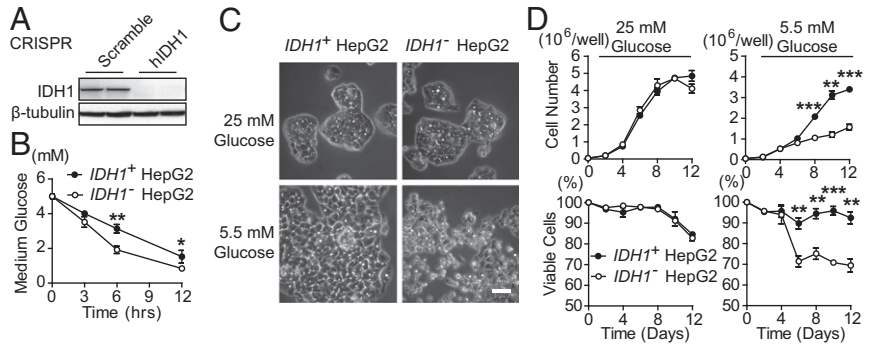

Fig. 3. Glucose stimulates heightened growth of *IDH1*-deficient HepG2 cells. (*A*) Immunoblot to detect IDH1 protein in two samples of *IDH1*-deficient (*IDH1*$^{-}$) HepG2 cells that were created by infecting HepG2 cells with human IDH1 CRISPR-Cas9 lentivirus. IDH1-expressing *IDH1*$^{+}$ HepG2 cells were created by infection with control Scramble CRISPR lentivirus. (*B*) Quantitation of glucose remaining in cultures of *IDH1*$^{+}$ and *IDH1*$^{-}$ HepG2 cells that were incubated in DMEM with 5.5 mM glucose for the indicated times. Data are the mean ± SEM ($n = 3$). (*C*) Phase contrast images of *IDH1*$^{+}$ and *IDH1*$^{-}$ HepG2 cells that were cultured (2×10^6 per well) for 24 h in DMEM supplemented with 5% dialyzed FBS plus 5.5 mM or 25 mM glucose. (Scale bar, 50 μm.) (*D*) Quantitation of (*Top*) total cell number and (*Bottom*) viability of *IDH1*$^{+}$ and *IDH1*$^{-}$ HepG2 cells that were cultured in six-well plates (5×10^4 per well) in DMEM supplemented with dialyzed 5% FBS plus 5.5 mM or 25 mM glucose for the indicated times. The medium was changed every other day, and cell numbers and viability were determined 24 h after the medium change. Data are the mean ± SEM ($n = 3$), $^{**}P < 0.01$, and $^{***}P < 0.001$ by Student's *t* test.

determined their viability. Both *IDH1*$^{+}$ and *IDH1*$^{-}$ HepG2 cells had similar rates of viability in control cultures containing DMEM supplemented with glucose and FBS, but neither line could survive in medium lacking both FBS and glucose, even when supplemented with glutamine, glutamate, aspartate, BCAA, or proline (Fig. 5*D* and Fig. S4*C*). Although *IDH1*$^{+}$ HepG2 cells were able to grow in FBS-free DMEM containing alanine, *IDH1*$^{-}$ HepG2 cells could not (Fig. 5*D*). Pyruvate, a downstream metabolite of alanine, could partially rescue the growth of *IDH1*$^{-}$ HepG2 cells in DMEM without glucose or FBS (Fig. 5*D*, *Right*). Thus, IDH1 is vital for alanine catabolism.

IDH1 Deficiency Attenuates Gluconeogenesis in Liver. In the liver, alanine's amino groups are transferred to α-KG by glutamate–pyruvate transaminase 1 (GPT1) to generate pyruvate and glutamate. Glutamate is then converted to α-KG in mitochondria via deamination by GLUD1. We found that ammonia production was decreased significantly in *IDH1*$^{-}$ HepG2 cells compared with *IDH1*$^{+}$ HepG2 cells when cultured in medium containing 10 mM alanine (Fig. 6*A*). In cultured WT and *IDH1*-null primary hepatocytes, the addition of excess glutamine and alanine increased ammonia production by both lines, but this increase was ~30% lower in the mutant cells when the DMEM contained 10 mM glutamine and ~40% lower in the presence of 10 mM alanine (Fig. 6*B*). Thus, IDH1 is required for normal AA utilization.

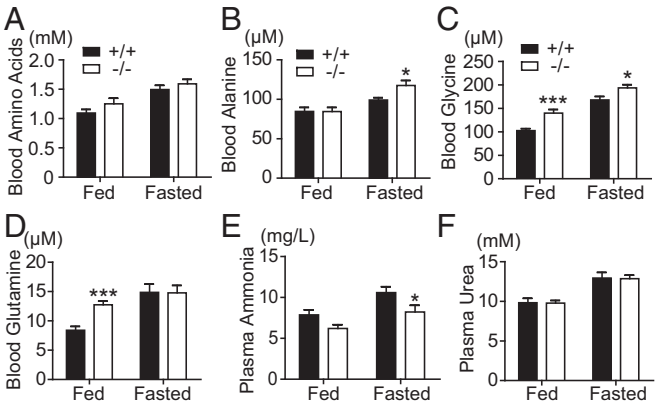

Fig. 4. Increased blood amino acid levels in *IDH1*-null mice. Quantitation of blood levels of (*A*) total AAs, (*B*) alanine, (*C*) glycine, and (*D*) glutamine in 12-wk-old WT ($n = 8$) and *IDH1*-null ($n = 8$) mice that were ND fed or fasted for 24 h. Fresh blood was collected by cardiac puncture and analyzed by LC/MS-MS. For other blood AAs, please see Table S1. Quantitation of (*E*) serum ammonia and (*F*) urea in the mouse blood samples in *A*–*D*. Data are the mean ± SEM ($n = 8$). For *B*–*E*, $^{*}P < 0.05$ and $^{***}P < 0.001$ by Student's *t* test.

Ammonia produced by AA deamination is converted to urea via the hepatic urea cycle. We found that urea production was decreased in *IDH1*-null primary hepatocytes by only ~10% compared with WT controls (Fig. 6*C*). Pyruvate is generated from alanine by α-KG transamination mediated by GPT1, and pyruvate is a major substrate for gluconeogenesis. Glucose output was decreased by ~25% in *IDH1*-null primary hepatocytes cultured in medium with 10 mM alanine, but this deficit could be eliminated by treatment of the cells with L-cycloserine (L-CS), an inhibitor of GPT1 (Fig. 6*D*). Thus, IDH1 is critical for AA utilization leading to gluconeogenesis.

We next used microarray to determine gene expression patterns in *IDH1*-deficient liver. The mRNAs for enzymes involved in transamination or deamination, such as GPT1, glutaminase 2 (GLS2), and GLUD1, were decreased in *IDH1*-null liver, whereas mRNAs for enzymes involved in gluconeogenesis, such as fructose bisphosphatase 1 (FBP1), FBP2, and glucose-6-phosphatase, catalytic subunit (G6PC3), were increased (Fig. 7*A*). Notably, mRNAs of IDH2, IDH3, and enzymes participating in the urea cycle or lipid biosynthesis were not altered in *IDH1*-null livers (Fig. 7*A*). Quantitative PCR showed that the mRNA levels of GPT1, branched chain amino acid transaminase 1 (BCAT1), GLS2, and GLUD1 were decreased in *IDH1*-null livers compared with WT livers (Fig. 7*B*), suggesting impaired transamination and deamination in the absence of IDH1. However, the mRNA levels of PCK1, FBP1/2, G6PC, and G6PC3 were increased in *IDH1*-null livers (Fig. 7*B*), indicating that genes involved in gluconeogenesis were up-regulated due to a decrease in glucogenic substrates. Last, determination of intracellular α-KG and glutamate levels showed that both of these molecules were decreased in *IDH1*-null primary hepatocytes cultured in medium containing 10 mM alanine (Fig. 7 *C* and *D*). These data suggest that IDH1 deficiency reduces gluconeogenesis by impairing the utilization of AAs such as alanine.

Discussion

IDH1 is a cytosolic enzyme that converts isocitrate to α-KG while reducing $NADP^{+}$ to NADPH (15). It was recently reported that IDH1 protects murine hepatocytes from endotoxin-induced oxidative stress by regulating the intracellular $NADP^{+}$/NADPH ratio (12). Because NADPH is a major cofactor for fatty acid biosynthesis, IDH1 transgenic mice showed markedly higher liver and serum levels of total TG and cholesterol compared with WT mice, suggesting that IDH1 might be a major NADPH producer for lipid biosynthesis (7). Others have found that IDH1 mediates reductive glutamine metabolism for lipogenesis in hypoxic cells (9). However, we have shown here that *IDH1*-null mice have normal body weights and hepatic lipid contents, although WAT was slightly decreased in ND-fed *IDH1*-null mice.

In this study, we observed that the body weight of *IDH1*-null mice was slightly lower than wild-type mice when fed with a 50% protein diet and that fasting blood glucose was decreased in

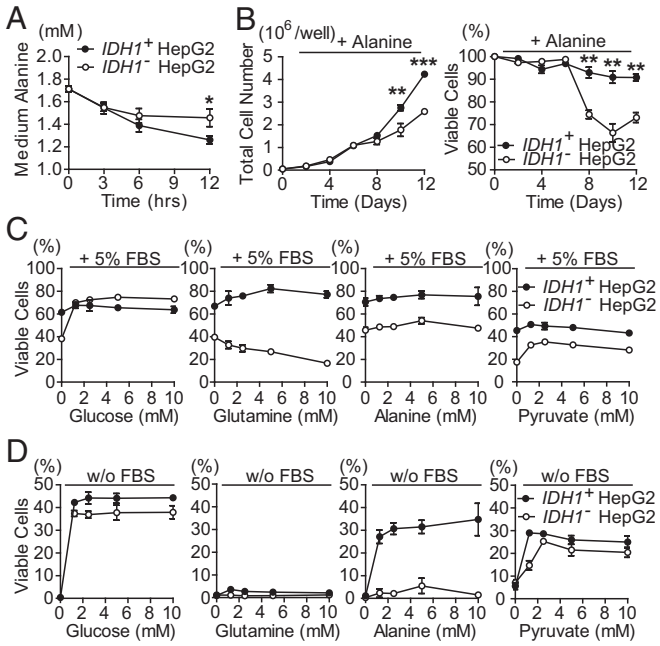

Fig. 5. Attenuated utilization of amino acids by *IDH1*-deficient HepG2 cells. (*A*) Quantitation of residual alanine after *IDH1*$^+$ and *IDH1*$^-$ HepG2 cells were cultured in DMEM with 5 mM alanine for the indicated times. Data are the mean ± SEM ($n = 3$). (*B*) Quantitation of (*Left*) total cell numbers and (*Right*) viability of *IDH1*$^+$ and *IDH1*$^-$ HepG2 cells that were cultured (5×10^4 per well) in medium supplemented with 10 mM alanine for the indicated times. Data are the mean ± SEM ($n = 3$). (*C*) Quantitation of viable cells in cultures of *IDH1*+ and *IDH1*$^-$ HepG2 cells that were incubated in medium containing 5% dialyzed FBS plus the indicated concentrations of glucose, glutamine, alanine or pyruvate. After 16 h, viable cells were detected by crystal violet staining. For other AAs, please see Fig. S4*B*. (*D*) Quantitation of viable cells in cultures of *IDH1*$^+$ and *IDH1*$^-$ HepG2 cells that were cultured in DMEM lacking FBS but supplemented with the indicated concentrations of glucose, glutamine, alanine, or pyruvate. Viability was determined as in *C*. For other AAs, please see Fig. S4*C*. Data are the mean ± SEM ($n = 3$). For *A* and *B*, $^*P < 0.05$, $^{**}P < 0.01$, and $^{***}P < 0.001$ by Student's *t* test.

IDH1-null mice. In the future, it will be interesting to examine the effects of additional dietary stresses in *IDH1*-null mice, including further reduction in carbohydrate intake in the context of a high-protein diet. To further investigate these in vivo data, we found that *IDH1*$^-$ HepG2 cells could not survive in low-glucose medium and that *IDH1*$^-$ HepG2 cells consumed more glucose than *IDH1*$^+$ HepG2 cells. This increased glucose consumption suggests that IDH1 deficiency impairs AA utilization, consistent with the slightly higher levels of blood AAs in *IDH1*-null mice compared with WT controls. Under fasting conditions, both blood alanine and glycine were increased in *IDH1*-null mice. Glutamine is synthesized mainly in skeletal muscle in vivo, but under prolonged fasting conditions, skeletal muscle switches to an alanine releasing phenotype to support gluconeogenesis in liver to maintain blood glucose. Our results show that blood glutamine was increased in *IDH1*-null mice only in the fed condition, which may relate to this metabolic switch. Moreover, *IDH1*$^-$ HepG2 cells consumed less alanine than *IDH1*$^+$ HepG2 cells, and excess alanine failed to improve the growth and viability of *IDH1*$^-$ HepG2 cells. When these cells were cultured in medium containing 5% FBS but lacking glucose, the viability of *IDH1*$^-$ HepG2 cells was not improved by AA addition, suggesting that the defect in AA metabolism was caused by IDH1 deficiency. This hypothesis was confirmed by the ability of alanine to support the growth of *IDH1*$^+$ HepG2 cells but not *IDH1*$^-$ HepG2 cells, in medium lacking both glucose and FBS. These data suggest that IDH1 deficiency increases glucose consumption while impairing AA utilization.

Glycogenolysis and gluconeogenesis contribute almost equally to hepatic glucose output in WT mice fasted overnight (16), but the glycogen stores in these animals are consumed within 36–48 h of fasting. When fasting is prolonged, alanine is formed (mainly from skeletal muscle) by transamination of glucose-derived pyruvate. This alanine is transported to the liver where its carbon backbone is used for gluconeogenesis to stabilize blood glucose levels, a process known as the glucose–alanine cycle (17). Our tissue distribution study showed that IDH1 expression is high in the liver but absent in skeletal muscle. After alanine is taken up by hepatocytes, it is converted to pyruvate by transamination via GPT1 and contributes to either gluconeogenesis, lipid biogenesis, or the Krebs cycle. In *IDH1*-null hepatocytes, α-KG production was reduced, alanine utilization was decreased, and GPT1 expression was down-regulated. Transamination of alanine converts α-KG to glutamate, which is deaminated by GLUD1 in mitochondria. GLUD1 is a mitochondrial matrix enzyme with a key role in nitrogen and glutamate metabolism. Ammonia produced by GLUD1 is converted to urea via the urea cycle. Therefore, we initially speculated that IDH1 deficiency might reduce gluconeogenesis from alanine by reducing α-KG–dependent transamination. However, we found that blood levels of free AAs were slightly increased in fasted *IDH1*-null mice when AA deamination was stimulated in the liver. These results suggested that mitochondrial α-KG might be transported into the cytosol to compensate for the decreased cytosolic α-KG in *IDH1*-null liver. Similarly, GLUD1 expression and production of ammonia and urea were all decreased only slightly in *IDH1*-deficient primary hepatocytes and *IDH1*$^-$ HepG2 cells, whereas urea cycle enzymes were unchanged or slightly altered.

In addition to the liver, IDH1 is highly expressed in kidney, intestinal mucosa, and adipose tissues, where transamination is also very active. Amino acids can be used for lipogenesis in adipose tissues, which might explain why these tissues need high levels of cytosolic IDH1 and why overexpression of IDH1 promotes lipogenesis in adipose tissues and livers of IDH1 transgenic mice (7). In contrast, in skeletal muscle and heart where cytosolic IDH1 is absent or very low, the mitochondrial α-KG is

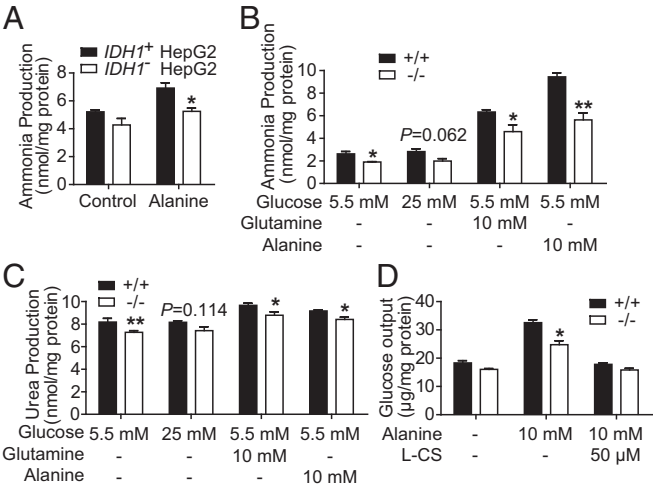

Fig. 6. IDH1 deficiency leads to defects in deamination and gluconeogenesis. (*A*) Quantitation of ammonia production by *IDH1*$^+$ and *IDH1*$^-$ HepG2 cells cultured for 2 h in DMEM with or without 10 mM alanine. Data are the mean ± SEM ($n = 3$). Quantitation of (*B*) free ammonia and (*C*) urea produced by WT ($^{+/+}$) and *IDH1*-null ($^{-/-}$) hepatocytes (5×10^5 cells per well) that were incubated in DMEM supplemented with glucose or AAs for 2 h and then cultured overnight in standard medium. Data are the mean ± SEM ($n = 3$). (*D*) Quantitation of glucose output by WT and *IDH1*-null primary hepatocytes (5×10^5cells per well) that were fasted for 6 h and then incubated for 2 h in DMEM supplemented with 10 mM alanine, with or without 50 μM L-cycloserine (L-CS, GPT inhibitor). Data are the mean ± SEM ($n = 3$). For *A–D*, $^*P < 0.05$ and $^{**}P < 0.01$ by Student's *t* test.

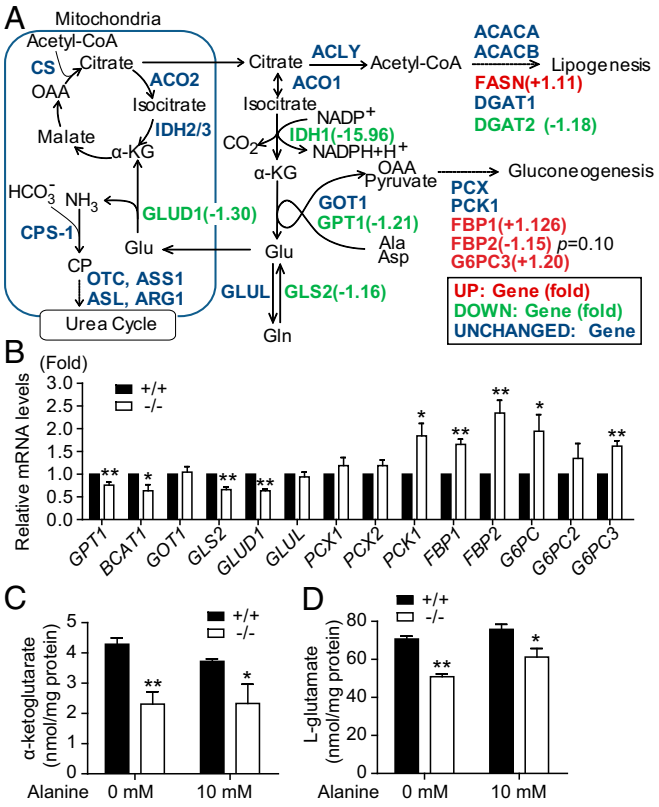

Fig. 7. Transamination in *IDH1*-deficient cells is impaired due to reduced α-KG generation. (*A*) Schematic diagram illustrating metabolic pathways in WT liver and mRNA levels of key enzymes in these pathways in *IDH1*-deficient livers as determined by microarray. Up-regulated mRNAs are shown in red, and down-regulated mRNAs are shown in green. (*B*) Quantitative PCR determination of mRNA levels of the indicated genes involved in AA metabolism and gluconeogenesis (primers used for qPCR were listed in Table S2). Data are expressed relative to levels in WT liver and are the mean ± SEM ($n = 3$). Quantitation of intracellular levels of (*C*) α-KG and (*D*) glutamate in $IDH1^+$ and $IDH1^-$ HepG2 cells cultured in DMEM lacking FBS and glucose but containing 10 mM alanine. Data are the mean ± SEM ($n = 3$). For *B–D*, $^*P < 0.05$ and $^{**}P < 0.01$ by Student's *t* test.

likely transported into the cytosol by the oxoglutarate carrier (OGC) SLC25A11 (18). However, the levels of SLC25A11 are relatively lower in liver, and compensation by mitochondrial α-KG for the deletion of cytosolic IDH1 may be limited. The Krebs cycle in liver mitochondria supplies the majority of intermediates for the cytosolic biosynthesis of lipids and AAs. It has been reported that proliferating mammary epithelial cells catabolize glutamate primarily via transaminases to synthesize nonessential AAs and generate α-KG, suggesting that cytosolic α-KG is critical for cell proliferation (19). Besides as an amino acceptor, α-KG is used as a cofactor for DNA modifying enzymes and histone demethylases, including ten–eleven translocation (TET) proteins and JmjC-domain containing histone demethylases (JHDM) (20, 21). Supplementation with α-KG decreases DNA methylation and histone methylation, increases stem cell self-renewal, and suppresses cell differentiation (22). Therefore, further studies are required to delineate the effects of IDH1 deficiency on the epigenetic state of specific cell types.

Citrate is generated in the mitochondria, but it is an important substrate for biosynthesis in the cytosol upstream of IDH1 (23). As a mitochondrial citrate carrier (CIC), SLC25A1 promotes the efflux of citrate from mitochondria into the cytosol (24–26), where it can be converted into oxaloacetate and acetyl-CoA by ATP citrate lyase (ACL) or into isocitrate by aconitase 1 (Aco1) and then oxidized by IDH1 to generate NADPH and α-KG. Both acetyl-CoA and NADPH are the substrates for lipid biosynthesis, which is critical for cell proliferation, and therefore, SLC25A1 is an important molecule upstream of IDH1. It was reported that SLC25A1 is a direct transcriptional target of several p53 mutants and that inhibition of CIC activity blunts mutant p53-driven tumor growth (27). Recessive mutations in the human *SLC25A1* gene cause D,L-2-HG aciduria (28). Although the origin of the D- and L-2-HG in these patients is still unclear, it may involve α-KG metabolism. Moreover, knockdown of *Aco1* in 3T3-L1 cells diminishes cytosolic Aco1 activity and *IDH1* mRNA levels and also impairs adipogenesis (29), which may be due to the impaired production of cytosolic α-KG. Collectively, these observations provide further evidence that IDH1 may have important functions related at least in part to its role in cytosolic α-KG metabolism.

IDH1/2 mutations occur in grade II~III glioma, secondary glioblastoma, acute myelogenous leukemia, enchondroma, and chondrosarcoma (30–33). Although mutant IDH1/2 enzymes have been widely studied, the biologic functions of WT IDH1 have been controversial despite the clarification of IDH1 enzymatic activity some decades ago. In our study, we have shown that the IDH1 product cytosolic α-KG is a key substrate for hepatic transamination and deamination and that IDH1 deficiency impairs hepatic gluconeogenesis by reducing alanine utilization. Thus, IDH1 is critical for normal AA utilization.

Materials and Methods

Mice. *IDH1*-null mice have been described previously (3). The WT and *IDH1*-null male mice used in this study were of the C57BL/6 genetic background. Mouse protocols were approved by the Animal Care Committees of the University Health Network (Canada) or the Fourth Military Medical University (China). Mice were housed four to five per cage in an animal room with a 12-h on/off light cycle and free access to drinking water and mouse chow. WT and *IDH1*-null mice (4 wk old; $n = 8$ per group) were fed an ND of standard mouse chow (TD.91352; Teklad Laboratory) or an HPD (TD.90018; Teklad Laboratory) for 8 wk. Body weights were monitored 2 times per wk. Mice were killed at age 12 wk, and epididymal, inguinal, and perirenal WAT were dissected and weighed.

For fasting experiments, chow was removed, but water was provided ad libitum. Mice were killed by CO_2 asphyxiation within 24 h of showing early signs of health deterioration, i.e., before exhibiting significant distress. The humane endpoint was defined as body weight loss >20% relative to initial weight, accompanied by hunched posture, lethargy, and poor grooming.

Primary Mouse Hepatocytes. Hepatocytes were isolated by the modified collagenase method as previously described (34).

Immunoblotting. Tissues or cell samples were homogenized in RIPA buffer containing protease inhibitor mixture (Roche). Immunoblots were visualized with horseradish peroxidase (HRP)-conjugated secondary Ab (Santa Cruz Biotechnology; 1:5,000) using enhanced chemiluminescence (Millipore). Primary Abs were anti-IDH1 (goat polyclonal; Santa Cruz Biotechnology; 1:2,000), anti-acetyl-CoA carboxylase (ACC) (rabbit monoclonal; Cell Signaling Technology; 1:1,000), and anti-β-tubulin (mouse monoclonal; Cell Signaling Technology; 1:1,000).

Generation of *IDH1*-Deficient HepG2 Cells. CRISPR-Cas9 was used to generate *IDH1*-deficient ($IDH1^-$) HepG2 cells. Briefly, DNA fragments 5′-CACCGTGTAGATCCAATTCCACGTA-3′ and 5′-AAACTACGTGGAATTGGATCTACAC-3′ were annealed and treated with T4 kinase. The annealed DNA fragment was subcloned between *Bsm*BI sites of LentiCRISPR vector to generate sgRNA targeted on human IDH1 (5′-TGTAGATCCAATTCCACGTA-3′) (14). IDH1 CRISPR lentivirus was generated by transfecting LentiCRISPR-hIDH1, psAX2, and pVSVG plasmids into 293T cells. HepG2 cells were infected with IDH1 CRISPR lentivirus and selected by growth in 2 μg/mL puromycin for 2 wk. IDH1 expression was measured by immunoblotting as above. An sgRNA targeting EGFP was used to generate control ($IDH1^+$) HepG2 cells.

LC-MS/MS Measurement of Blood Amino Acids. Mouse blood was dropped directly onto filter paper (Whatman) without additives and dried at room temperature. Determination of AAs from filter papers was performed using HPLC (LC; Shimadzu SI20AC) and tandem mass spectrometry (API 4000plus; AB SCIEX) as previously described (35). Data processing and calculations were performed with ChemoView Software (AB SCIEX).

Ammonia and Urea Determinations. For plasma determinations, blood samples of killed mice were obtained by cardiac puncture. Plasma was separated, and

ammonia and urea concentrations were determined using commercial ammonia and urea assay kits (Sigma) according to the manufacturer's instructions. Absorbance at 340 nm was measured with a spectrophotometer (FlexStation 3; Molecular Devices).

For primary hepatocytes, cells (5×10^5) were plated in 35-mm dishes and cultured overnight. Fresh DMEM (A14430-01; Gibco) supplemented with 5.5 mM glucose, 25 mM glucose, 10 mM glutamine, or 10 mM alanine (as indicated in Fig. 6 *B* and *C*) was added to cultures, and ammonia and urea production were measured colorimetrically after 2 h using kits (Sigma) according to the manufacturer's instructions.

For ammonia generated by HepG2 cells, *IDH1*$^+$ and *IDH1*$^-$ HepG2 cells were cultured in 35-mm dishes to 90% confluence. The medium was changed to DMEM (A14430-01; Gibco) with and without 10 mM alanine. Ammonia produced was measured after 2 h using the kits described above.

Endogenous Glucose Production. Primary mouse hepatocytes were cultured in six-well plates overnight. Cells were then pretreated for 6 h with DMEM lacking FBS and glucose, after which 10 mM alanine was added as a gluconeogenic substrate for 2 h. Glucose production in the medium was measured using an endpoint fluorimeter-coupled enzyme assay kit (Abcam).

Glutamate and α-KG Measurements. *IDH1*$^+$ and *IDH1*$^-$ HepG2 cells were cultured in 35-mm dishes to 80% confluence. The medium was changed to DMEM (A14430-01; Gibco) supplemented with 10 mM glucose and 5% FBS for 12 h, followed by culture in DMEM (A14430-01; Gibco) supplemented with and without 10 mM alanine for 6 h. Intracellular glutamate and α-KG were measured colorimetrically using a glutamate assay kit (ab83389; Abcam) and an α-KG assay kit (ab83431; Abcam) according to the manufacturer's instructions.

Growth Curves and Viability. To determine the effect of glucose concentration on the growth and viability of HepG2 cells, *IDH1*$^+$ and *IDH1*$^-$ HepG2 cells were inoculated in six-well plates (5×10^4 per well) and cultured in DMEM (A14430-01; Gibco) containing 5% dialyzed FBS (HyClone) plus 5.5 or 25 mM glucose. To determine the effects of alanine and glutamine on HepG2 cell growth, DMEM containing 5% dialyzed FBS plus 10 mM alanine or 10 mM glutamine was used. The medium was changed every other day, and cell numbers and viability were measured 24 h after each medium change using a Beckman Coulter Vi-CELL XR Cell Viability Analyzer.

Crystal Violet Staining. *IDH1*$^+$ and *IDH1*$^-$ HepG2 cells (1.5×10^4 per well) were inoculated in flat bottom 96-well plates and incubated at 37 °C in 5% CO_2 overnight. After washing with PBS, cells were incubated for 12 h in DMEM (A14430-01; Gibco; without glucose, glutamine, alanine, or pyruvate) with and without 5% dialyzed FBS and various concentrations of glucose, alanine, glutamine, glutamate, proline, or BCAA (ratio of leucine:isoleucine:valine = 2:1:1). After removal of medium, cells were fixed in 100 μL 4% paraformaldehyde followed by staining in 100 μL 0.5% crystal violet (Sigma) in 20% methanol for 2 h. The stain was removed by rinsing in water, and the plates were dried. Crystal violet was extracted from live cells with 100 μL methanol, and absorbance at 595 nm was measured with a spectrophotometer (FlexStation 3; Molecular Devices). *IDH1*$^+$ HepG2 cells cultured in DMEM supplemented with 5% dialyzed FBS, 5.5 mM glucose, and 2 mM glutamine were assayed as a control.

Histological Analysis. Mouse tissues were fixed overnight at 4 °C in PBS-buffered 4% (wt/vol) paraformaldehyde and embedded in paraffin. Cross-sections (5 μm) were prepared for hematoxylin-eosin (HE) and Periodic acid–Schiff (PAS) staining. For Oil Red O staining, mice were killed, and livers were immediately removed, cut into 10-μm sections, and fixed in 4% formaldehyde for 10 min. Sections were stained with 0.5% (wt/vol) Oil Red O solution in 60% isopropanol for 30 min, washed briefly with 60% isopropanol and PBS, and counterstained with hematoxylin before microscopy. Cellular lipids were detected by staining with Bodipy 493/503 (Invitrogen).

Statistical Analysis. All results are presented as the mean ± SEM of at least three independent experiments, each performed in duplicate or triplicate. Data were analyzed by the two-sided Student's *t* test using Prism 5.0 software (GraphPad Prism). Differences of $P < 0.05$ were considered statistically significant. *P* values are $^*P < 0.05$, $^{**}P < 0.01$, and $^{***}P < 0.001$.

ACKNOWLEDGMENTS. We are grateful for the administrative assistance of Irene Ng and scientific editing of the manuscript by Mary Saunders. Research reported in this publication was supported in part by a grant to T.W.M. and R.A.C. from the Canadian Institutes of Health Research (MOP-125884) and to J.Y. from the National Natural Science Foundation of China (81572471 and 81370958).

1. Reitman ZJ, Yan H (2010) Isocitrate dehydrogenase 1 and 2 mutations in cancer: Alterations at a crossroads of cellular metabolism. *J Natl Cancer Inst* 102(13):932–941.
2. Hirata M, et al. (2015) Mutant IDH is sufficient to initiate enchondromatosis in mice. *Proc Natl Acad Sci USA* 112(9):2829–2834.
3. Sasaki M, et al. (2012) IDH1(R132H) mutation increases murine haematopoietic progenitors and alters epigenetics. *Nature* 488(7413):656–659.
4. Cairns RA, et al. (2012) IDH2 mutations are frequent in angioimmunoblastic T-cell lymphoma. *Blood* 119(8):1901–1903.
5. Lazarow PB (1987) The role of peroxisomes in mammalian cellular metabolism. *J Inherit Metab Dis* 10(Suppl 1):11–22.
6. Shechter I, Dai P, Huo L, Guan G (2003) IDH1 gene transcription is sterol regulated and activated by SREBP-1a and SREBP-2 in human hepatoma HepG2 cells: Evidence that IDH1 may regulate lipogenesis in hepatic cells. *J Lipid Res* 44(11):2169–2180.
7. Koh HJ, et al. (2004) Cytosolic NADP+-dependent isocitrate dehydrogenase plays a key role in lipid metabolism. *J Biol Chem* 279(38):39968–39974.
8. Mullen AR, et al. (2011) Reductive carboxylation supports growth in tumour cells with defective mitochondria. *Nature* 481(7381):385–388.
9. Metallo CM, et al. (2011) Reductive glutamine metabolism by IDH1 mediates lipogenesis under hypoxia. *Nature* 481(7381):380–384.
10. Filipp FV, Scott DA, Ronai ZA, Osterman AL, Smith JW (2012) Reverse TCA cycle flux through isocitrate dehydrogenases 1 and 2 is required for lipogenesis in hypoxic melanoma cells. *Pigment Cell Melanoma Res* 25(3):375–383.
11. Leonardi R, Subramanian C, Jackowski S, Rock CO (2012) Cancer-associated isocitrate dehydrogenase mutations inactivate NADPH-dependent reductive carboxylation. *J Biol Chem* 287(18):14615–14620.
12. Itsumi M, et al. (2015) Idh1 protects murine hepatocytes from endotoxin-induced oxidative stress by regulating the intracellular NADP(+)/NADPH ratio. *Cell Death Differ* 22(11):1837–1845.
13. Morens C, et al. (2000) A high-protein meal exceeds anabolic and catabolic capacities in rats adapted to a normal protein diet. *J Nutr* 130(9):2312–2321.
14. Cong L, et al. (2013) Multiplex genome engineering using CRISPR/Cas systems. *Science* 339(6121):819–823.
15. Haselbeck RJ, McAlister-Henn L (1993) Function and expression of yeast mitochondrial NAD- and NADP-specific isocitrate dehydrogenases. *J Biol Chem* 268(16):12116–12122.
16. Klover PJ, Mooney RA (2004) Hepatocytes: Critical for glucose homeostasis. *Int J Biochem Cell Biol* 36(5):753–758.
17. Felig P (1973) The glucose-alanine cycle. *Metabolism* 22(2):179–207.
18. Lash LH (2006) Mitochondrial glutathione transport: Physiological, pathological and toxicological implications. *Chem Biol Interact* 163(1-2):54–67.
19. Coloff JL, et al. (2016) Differential glutamate metabolism in proliferating and quiescent mammary epithelial cells. *Cell Metab* 23(5):867–880.
20. Wu H, Zhang Y (2014) Reversing DNA methylation: Mechanisms, genomics, and biological functions. *Cell* 156(1-2):45–68.
21. Lu C, Thompson CB (2012) Metabolic regulation of epigenetics. *Cell Metab* 16(1):9–17.
22. Carey BW, Finley LW, Cross JR, Allis CD, Thompson CB (2015) Intracellular α-ketoglutarate maintains the pluripotency of embryonic stem cells. *Nature* 518(7539):413–416.
23. Catalina-Rodriguez O, et al. (2012) The mitochondrial citrate transporter, CIC, is essential for mitochondrial homeostasis. *Oncotarget* 3(10):1220–1235.
24. Gutiérrez-Aguilar M, Baines CP (2013) Physiological and pathological roles of mitochondrial SLC25 carriers. *Biochem J* 454(3):371–386.
25. Palmieri F (2013) The mitochondrial transporter family SLC25: Identification, properties and physiopathology. *Mol Aspects Med* 34(2-3):465–484.
26. Palmieri F (2014) Mitochondrial transporters of the SLC25 family and associated diseases: a review. *J Inherit Metab Dis* 37(4):565–575.
27. Kolukula VK, et al. (2014) SLC25A1, or CIC, is a novel transcriptional target of mutant p53 and a negative tumor prognostic marker. *Oncotarget* 5(5):1212–1225.
28. Nota B, et al. (2013) Deficiency in SLC25A1, encoding the mitochondrial citrate carrier, causes combined D-2- and L-2-hydroxyglutaric aciduria. *Am J Hum Genet* 92(4):627–631.
29. Moreno M, et al. (2015) Cytosolic aconitase activity sustains adipogenic capacity of adipose tissue connecting iron metabolism and adipogenesis. *FASEB J* 29(4):1529–1539.
30. Cairns RA, Mak TW (2013) Oncogenic isocitrate dehydrogenase mutations: Mechanisms, models, and clinical opportunities. *Cancer Discov* 3(7):730–741.
31. Parsons DW, et al. (2008) An integrated genomic analysis of human glioblastoma multiforme. *Science* 321(5897):1807–1812.
32. Ward PS, et al. (2010) The common feature of leukemia-associated IDH1 and IDH2 mutations is a neomorphic enzyme activity converting alpha-ketoglutarate to 2-hydroxyglutarate. *Cancer Cell* 17(3):225–234.
33. Amary MF, et al. (2011) IDH1 and IDH2 mutations are frequent events in central chondrosarcoma and central and periosteal chondromas but not in other mesenchymal tumours. *J Pathol* 224(3):334–343.
34. Wang C, et al. (2015) Perilipin 5 improves hepatic lipotoxicity by inhibiting lipolysis. *Hepatology* 61(3):870–882.
35. Wang C, Zhang W, Song F, Liu Z, Liu S (2012) A simple method for the analysis by MS/MS of underivatized amino acids on dry blood spots from newborn screening. *Amino Acids* 42(5):1889–1895.